(i.e., std ($\hat{f}$) greater than about $0.1/T$) for reasons discussed earlier.

In the high SNR case defined by $3p\text{SNR}/N \gg 1$ we have from (2)

$$\text{std}(\hat{f}) \approx \frac{0.1 * 3^{0.87}}{N^{1.30}\text{SNR}^{0.37}} \tag{4}$$

and the p dependence disappears. This corresponds to the lowest curve segments on Fig. 1, which are severely flattened implying little variation with p. Again the relationship to the CRLB is interesting and is given by

$$\frac{\text{std}(\hat{f})}{\text{CRLB}(\hat{f})} \approx \frac{0.2\,\pi * 3^{0.87}}{\sqrt{6}} \cdot N^{0.2}\text{SNR}^{0.13}$$

which says, surprisingly, perhaps, that the Burg technique in the high SNR region deteriorates, though quite weakly, with both N and SNR as can be verified by inspection of Fig. 1.

Conclusion

The standard deviation of the Burg frequency estimate has been computed for the simplest case of a single noisy complex sinusoid through a Monte Carlo simulation for a useful range of data lengths, SNR's, and model orders. These results have been shown to be amenable to a fit by a simple expression which yields insight into the behavior of the Burg algorithm particularly in that it clearly demarcates regions of "high SNR" performance and "low SNR" performance (though the precise definitions of these regions include model order and data length). Additional insight is gained when this approximate expression is used in conjunction with the Cramer–Rao lower bound. It is felt that these results may be useful to those working in the general area of spectral estimation.

References

[1] M. Kaveh and G. A. Lipperat, "An optimum tapered Burg algorithm for linear prediction and spectral analysis," *IEEE Trans. Acoust., Speech, Signal Processing*, vol. ASSP-31, pp. 438–444, Apr. 1983.

[2] B. I. Helme and C. L. Nikias, "Improved spectrum performance via data-adaptive weighted Burg technique," *IEEE Trans. Acoust., Speech, Signal Processing*, vol. ASSP-33, pp. 903–910, Aug. 1985.

[3] S. L. Marple, *Digital Analysis with Applications.* Englewood Cliffs, NJ: Prentice-Hall, 1987.

[4] W. A. Gardner, *Statistical Spectral Analysis: A Nonprobablistic Approach.* Englewood Cliffs, NJ: Prentice-Hall, 1988.

[5] R. Kumaresan and D. W. Tufts, "Estimating the parameters of exponentially damped simusoids and pole-zero modeling in noise," *IEEE Trans. Acoust., Speech, Signal Processing*, vol. ASSP-30, pp. 833–840, Dec. 1982.

Comments on "Classification of Natural Textures by Means of Two-Dimensional Orthogonal Masks"

Michael Unser

***Abstract*—The correspondence of Cohen *et al.* describes a texture analysis method that is a special use of the approach reported in [3]. Moreover, the derivation of the optimum set of masks presented by these authors is based on an incorrect assumption; the correct solution should be the local Karhunen–Loève transform which is generally different from a 2 × 2 Hadamard transform (2 × 2 DHT). However, this error has relatively minor effects from a practical point of view since the ability of the 2 × 2 DHT to decorrelate real texture images is usually excellent.**

Manuscript received March 9, 1990; revised July 13, 1990.

The author is with the Biomedical Engineering and Instrumentation Program, National Institutes of Health, Bethesda, MD 20892.

IEEE Log Number 9042288.

In a recent correspondence, Cohen *et al.*[1] describe a texture classification technique using features derived from a set of 4 orthogonal masks applied to a 2 × 2 local neighborhood that is an extension of the sum and difference histograms method [1]. A technique that is more general and subsumes the results of Cohen *et al.* and Unser [1] has been derived and is described in [2] and [3]. A procedure for deriving convolution masks that are optimal for texture analysis and classification is contained in [3].

For texture analysis, the optimal solution is provided by the Karhunen–Loève transform associated with the spatial covariance matrix of the texture being analyzed. For a two class texture classification problem, the set of masks providing maximal texture discrimination is determined by simultaneously diagonalizing the two corresponding covariance matrices. Since these solutions are texture dependent, it has been suggested that suboptimal transforms be used, e.g., the discrete cosine (DCT), discrete sine (DST), discrete real even Fourier (DREFT), and discrete real odd Fourier (DROFT), and discrete Hadamard (DHT) transforms. These results apply for rectangular neighborhoods of any size. In the particular case of a 2 × 2 neighborhood, these transformations are all equivalent to the 2 × 2 DHT: the transformation used by Cohen *et al.* It is reassuring to note that these authors have conducted experiments, obtaining results that are virtually identical to those presented in [3]. This latter study reported on experiments carried out with larger neighborhoods (3 × 3, 4× 4, and 5 × 5), and with a variety of different operator sets and textures features as well.

We also note that there is a mathematical error in the work by Cohen *et al.* although, from a practical point of view, it is likely to have minor effects. The general form of the spatial covariance matrix associated with the four pixel neighborhood vector $\boldsymbol{x}_{i,j} = [x_{i-1,j-1}x_{i-1,j}x_{i,j-1}x_{i,j}]^T$ where $\{x_{i,j}, (i = 1, \cdots, I; j = 1, \cdots, J)\}$ is a realization of a two-dimensional stationary and ergodic process, is

$$\boldsymbol{R}_x = E\left\{[x - E\{x\}][x - E\{x\}]^T\right\}$$

$$= \sigma^2 \begin{bmatrix} 1 & \rho_{90} & \rho_0 & \rho_{135} \\ \rho_{90} & 1 & \rho_{45} & \rho_0 \\ \rho_0 & \rho_{45} & 1 & \rho_{90} \\ \rho_{135} & \rho_0 & \rho_{90} & 1 \end{bmatrix} \tag{1}$$

in which $\sigma^2 = \text{var}\{x\}$ is the image variance, and where ρ_0, ρ_{45}, ρ_{90}, and ρ_{135} are the correlation coefficients in the four orientations schematically represented in Fig. 1. This expression differs from (2) in the correspondence by Cohen *et al.*; these authors have not distinguished between left and right diagonal interactions, which are not necessarily equal. It follows that $\boldsymbol{R}_x$ is, in general, not exactly diagonalized by the discrete Hadamard transformation (DHT), contrary to what has been stated by Cohen *et al.* This condition is only met when $\rho_{135} = \rho_{45}$, in which case $\boldsymbol{R}_x$ is dyadic, or when the covariance is separable along the two principal directions, which

[1] P. Cohen, C. T. DeDinh, and V. Lacasse, *IEEE Trans. Acoust., Speech, Signal Processing* (Correspondence), vol. 37, no. 1, pp. 125–128, Jan. 1989.

1053-587X/91/0400-1005$01.00 © 1991 IEEE

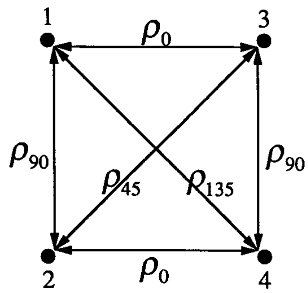

Fig. 1. Pairwise interactions between the four components of the local feature vector.

is a slightly more restrictive constraint:

$$R_x = \sigma^2 \begin{bmatrix} 1 & \rho_{90} \\ \rho_{90} & 1 \end{bmatrix} \otimes \begin{bmatrix} 1 & \rho_0 \\ \rho_0 & 1 \end{bmatrix} = \sigma^2 \begin{bmatrix} 1 & \rho_{90} & \rho_0 & \rho_0\rho_{90} \\ \rho_{90} & 1 & \rho_0\rho_{90} & \rho_0 \\ \rho_0 & \rho_0\rho_{90} & 1 & \rho_{90} \\ \rho_0\rho_{90} & \rho_0 & \rho_{90} & 1 \end{bmatrix}. \quad (2)$$

We note that this latter case corresponds to the direct separable extension of the results reported in [1], since the 2×2 DHT can be constructed from the outer product of horizontal and vertical one-dimensional sum and difference operators. The ability of the 2×2 DHT to decorrelate real texture images is usually excellent and is sufficient for most practical purposes. For instance, it was shown in [4] that the 2×2 DHT as applied to each of 12 Brodatz textures of an experimental set almost identical to that used by Cohen *et al.*, reduces the nondiagonal energy of the covariance matrix to less than 1% (with one exception at 2.2%) of its initial contribution.

References

[1] M. Unser, "Sum and difference histograms for texture classification," *IEEE Trans. Patt. Anal. Mach. Intell.*, vol. PAMI-8, pp. 118-125, Jan. 1986.
[2] M. Unser, "Local linear transforms for texture analysis," in *Proc. Seventh Int. Conf. Patt. Recog.* (Montreal, Canada), July 30-Aug. 2, 1984, pp. 1206-1208.
[3] M. Unser, "Local linear transforms for texture measurements," *Signal Processing*, vol. 11, pp. 61-79, July 1986.
[4] M. Unser, "Description statistique de textures: Application à l'inspection automatique," Ph.D. dissertation 534, Swiss Federal Inst. Technology, Lausanne, Switzerland, 1984.

On Coefficient-Quantization and Computational Roundoff Effects in Lossless Multirate Filter Banks

P. P. Vaidyanathan

Abstract—**FIR lossless transfer matrices have found recent applications in multirate analysis/synthesis systems having the perfect reconstruction property. It is shown in this correspondence that these lossless systems can be implemented such that regardless of coefficient quantization, the lossless property (and hence perfect reconstruction) can be retained. Such a result was shown to be true in the past only for two-channel filter banks. This correspondence also presents a noise gain result for lossless systems which finds application in analyzing roundoff noise in multirate filter banks.**

Manuscript received September 9, 1989; revised July 23, 1990. This work was supported in part by the National Science Foundation under Grants DCI8552579 and MIP8604456.

The author is with the Department of Electrical Engineering, California Institute of Technology, Pasadena, CA 91125.

IEEE Log Number 9042289.

I. Introduction

Multirate filter banks with the perfect reconstruction property have received considerable attention recently (see [1]-[7] and references therein). In this correspondence we are concerned with the technique reported in [3]-[7], in which the polyphase matrix of the set of analysis filters is FIR and lossless. Our purpose here is to present two results, one concerning coefficient quantization and the other concerning roundoff noise propagation.

Unless mentioned otherwise, the notations used are the same as those in any one of the [3]-[7]. As a review, $H_k(z)$ and $F_k(z)$, $0 \le k \le M - 1$ represent the M analysis and synthesis filters of an M band maximally decimated filter bank [6, fig. 1]. The analysis and synthesis banks are associated with two $M \times M$ matrices $\boldsymbol{E}(z)$ and $\boldsymbol{R}(z)$ called polyphase component matrices [6, fig. 2]. The methods employed in [3]-[7] are such that $\boldsymbol{E}(z)$ is (FIR and) lossless. This means that $\boldsymbol{E}(z)$ satisfies

$$\tilde{\boldsymbol{E}}(z)\,\boldsymbol{E}(z) = c^2\boldsymbol{I}, \qquad \forall z, \qquad c \text{ real.} \quad (1)$$

With $\boldsymbol{E}(z)$ satisfying this property, the maximally decimated system has perfect reconstruction if and only if the synthesis filters are chosen as $F_k(z) = \alpha z^{-L}\tilde{H}_k(z)$ where $\alpha \neq 0$ and L is an arbitrary integer.

If $c^2 = 1$ in (1), we say that $\boldsymbol{E}(z)$ is normalized-lossless. Note that losslessness can also be defined for rectangular matrices [5]. For $M \times 1$ stable systems, losslessness is same as the power-complementary property [7].

In order to design and implement filter banks with lossless $\boldsymbol{E}(z)$, it is necessary to obtain a structure for $M \times M$ FIR lossless systems. Structures for arbitrary real-coefficient FIR lossless systems were presented in [5] based on a state-space approach, with planar rotations as building blocks. More recently, a method was developed in [6] which leads to a different representation of lossless systems. This method does not involve rotations, but is entirely in terms of diadics (i.e., matrices of the form $\boldsymbol{v}\boldsymbol{v}^\dagger$ where $\boldsymbol{v}$ in a column vector). This is simpler in terms of derivation as well as implementation. Also, it covers both real and complex coefficient FIR lossless systems. In this correspondence, we shall show that the diadic based structure retains losslessness in spite of coefficient quantization (for arbitrary M), whereas such a property is not true for the rotation based structure except in the $M = 2$ case.

It should be noticed that the above discussion does not take into account errors due to quantization of signals (such as state variables) in the structure. The noise due to this must be separately analyzed; thus in Section IV we present a result on noise amplification by lossless systems, and indicate applications in filter bank structures.

II. Coefficient Quantization in Rotation-Based Structures

First consider a degree-0 lossless system $\boldsymbol{R}$ (i.e., a constant unitary matrix). The unitary property is equivalent to

$$\boldsymbol{R}_k^\dagger \boldsymbol{R}_m = 0, \qquad k \neq m \quad (2)$$

$$\boldsymbol{R}_m^\dagger \boldsymbol{R}_m = d > 0 \quad (3)$$

where $\boldsymbol{R}_m$ is the mth column of $\boldsymbol{R}$. Such matrices can be expressed in terms of planar rotations [8]. For example, in the 3×3 real-